



Observations of the Crab Nebula and Pulsar with VERITAS

O. CELIK¹, FOR THE VERITAS COLLABORATION²

¹University of California, Los Angeles, ²For full author list see G. Maier, "Status and Performance of VERITAS", these proceedings

celik@astro.ucla.edu

Abstract: Observations of the Crab Nebula have proven to be the best tool to calibrate and to characterize the performance of a Cherenkov telescope. Scientifically, it is interesting to measure the energy spectrum of the Crab Nebula close to the inverse-Compton peak where a deviation is expected from the power law seen at energies above 300 GeV. Additionally, it is important to search for pulsed emission from the Crab Pulsar at energies beyond the 10 GeV upper limit of the EGRET pulsar detection. Since current models predict a cut-off in pulsed emission between 10 and 100 GeV, measurements at energies close to this range may help to discriminate between them. We observed the Crab extensively in the 2006-2007 season during the VERITAS 2- and 3-telescope commissioning phases. Using this data set we reconstructed a preliminary energy spectrum of the signal from the Nebula. We also measured the optical pulsed signal to validate our GPS time-stamping and barycentering techniques and obtained an upper limit for the pulsed emission at gamma-ray energies.

Introduction

VERITAS, located in southern Arizona (32°N, 111°W) at an elevation of 1268 m, is an observatory designed to explore the very high energy (VHE) gamma-ray sky in the energy band between 100 GeV and 50 TeV [13]. It consists of four 12m diameter Cherenkov telescopes, each with a 499-pixel camera. It uses the stereoscopic imaging atmospheric Cherenkov technique (IACT) to detect gamma rays from astronomical sources. VERITAS has moved through phases of 2-, 3- and 4-telescope operation during its construction and commissioning this past year. We observed the Crab Nebula and Pulsar extensively during the 2- and 3-telescope phases. This paper discusses the analysis of these data. We also present a preliminary differential energy spectrum of the nebula and a preliminary upper limit for the pulsed gamma-ray emission.

The Crab Nebula and Pulsar

The Crab Nebula is a plerion-type supernova remnant (SNR). It was the first source definitively

detected at TeV energies, by the Whipple collaboration [16]. Its spectral energy distribution is well measured across a broad range of wavelengths and it is considered the standard candle in TeV astronomy due to its strong, stable emission. The nebula emission is believed to be powered by the conversion of the rotational slowdown of the central pulsar to synchrotron radiation. Inverse-Compton scattering of those synchrotron photons with the primary accelerated electrons gives rise to the emission in the gamma-ray regime as explained by the Synchrotron-Self-Compton model [6]. The Crab Nebula spectrum has been measured independently by many groups above ~ 200 GeV, with good agreement [9, 1, 15, 2]. Consistency with this established spectrum is an important test for any new gamma-ray telescope.

At the center of the Crab Nebula lies the Crab Pulsar (PSR 0531 +21). Periodic emission from the pulsar, with a 33 ms period, has been observed in all energy regimes with the exception of very high energy gamma rays. The EGRET detection of pulsed emission in the 100 MeV - 10 GeV energy band, with no evident turnover of its spectrum, is currently the highest energy detection [14]. None of the ground-based gamma-ray experiments sen-

sitive in the adjacent VHE domain has yet provided any detections. Currently there are two primary models attributing the pulsed emission to curvature and synchrotron radiation from the energetic electrons/positrons accelerated in the strong magnetic fields of the pulsar magnetosphere. These models differ by whether the emission region is near to the magnetic poles of the neutron star (the polar cap model [5]), or near to the light-cylinder at the outer magnetosphere (the outer gap model [10]). In the polar cap model, a super-exponential cut-off occurs in the pulsed spectrum at a few GeV due to the magnetic pair production in the strong field close to the pole. On the other hand, in the outer-gap model a cut-off at a few tens of GeV is expected due to photon-photon pair production, which has a weaker energy dependence. By detecting the pulsed emission or placing stringent upper limits in the GeV-TeV energy range, one can potentially discriminate between these models. VERITAS has a better sensitivity at lower energies than previous-generation IACT instruments. This suggests the possibility of detecting the pulsed emission, if an outer gap model applies, or of strongly constraining both models if pulsed emission is not detected.

Data Sample

The data set used in this analysis was selected from the observations made using 2 and 3 telescopes between October 2006 and February 2007. During that time, different trigger and observing configurations were tested to determine the optimum configuration for the array. Only data with this optimum configuration are used in the present analysis. Data-quality selection, based on the stability of trigger rates, response of the instrument to background cosmic rays and the deadtime of the system, was additionally used to reject low-quality data. The final data set, after this quality selection, is 15.7 hours of 2-telescope data and 3.3 hours of 3-telescope data. Data on both sets were collected in the so-called ‘‘wobble’’ observing mode, for which the telescopes are pointed such that the source is at a 0.5° offset from the position of the camera center. For 2-telescope data we required that both telescopes trigger within a certain coincidence time,

Quality Selection	Gamma/Hadron Separation
$Size > 400 \text{ dc.}$	$0.05 < MSW < 0.95$
$\#ofPix > 5$	$0.05 < MSL < 1.15$
$0.05^\circ < Dist. < 1.3^\circ$	$\theta^2 < 0.025$

Table 1: The standard cuts used in the analysis. The various quantities are defined in the text.

while for 3-telescope data we required that any two out of three telescopes trigger to record the event.

Analysis

The data were analyzed using the standard VERITAS analysis package [4, 3] in which calibration, cleaning and parametrization of the signal, reconstruction of the shower parameters and the gamma/hadron separation cuts are applied to the data. The cuts used in this analysis are listed in Table 1. The quality-selection cuts based on the total recorded signal ($Size$), the number of pixels in the image ($\#ofPix$) and the distance of its centroid from the center of the camera ($Dist.$) are applied before the stereo reconstruction. The gamma/hadron separation cuts based on the mean scaled width and length (MSW and MSL respectively) and the squared distance between the source and the reconstructed gamma ray position (θ^2) are applied at the final step. The same data were also analyzed using an independent analysis package to confirm the results.

Detection

The Crab Nebula is strongly detected during both 2-telescope and 3-telescope phases. The detection is at the $7 \gamma/\text{min}$ level with a significance of $31 \sigma/\sqrt{\text{hr}}$ for three telescopes and at $3.4 \gamma/\text{min}$ level with a significance of $20 \sigma/\sqrt{\text{hr}}$ for two telescopes using the cuts listed on Table 1. In the upper panel of Figure 1, the θ^2 distributions for the 2-telescope data (left) and the 3-telescope data (right) are shown. In the lower panel a sum of two Gaussian functions [2] is fit to the excess θ^2 distribution for each data set. The fit to 3-telescope data gives $A_{Rel} = 0.17$ with $\sigma_1 = 0.067$ and $\sigma_2 = 0.13$.

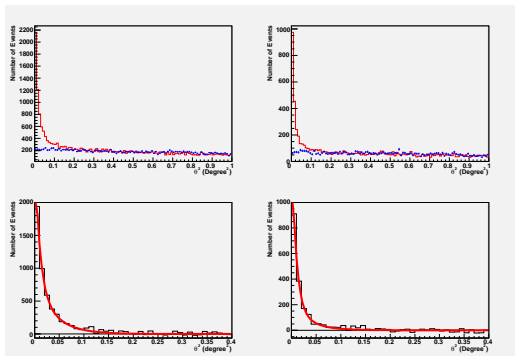


Figure 1: Theta-square distribution (upper) and its fit to a sum of two Gaussian functions (lower) for 2-telescope data (left) and 3-telescope data (right)

Spectrum

A preliminary Crab Nebula energy spectrum is reconstructed for events with energies between 300 GeV and 3 TeV. We are presently comparing our spectrum for consistency between two independent analysis packages developed for VERITAS. We will report our final result at the conference.

Temporal Analysis

The temporal analysis of the Crab signal is used to search for pulsed emission from the Crab Pulsar. The event arrival times are tagged online by GPS clocks at each telescope with precision of 100 ns. The GPS time of each event is transformed to the solar system barycenter to compensate for the motion of Earth. We then calculate the relative phase of the pulsar rotation for each event with respect to a reference epoch according to following equation.

$$\phi(T) = \phi(T_0) + f(T_0)(T - T_0) + \frac{1}{2}\dot{f}(T_0)(T - T_0)^2$$

The reference epoch is taken as the arrival time of the first radio pulse at the solar system barycenter. The radio ephemerides for the Crab pulsar are obtained from the Jodrell Bank Observatory [12]. Barycentering libraries used in this analysis were developed [7] and tested for this analysis using the optical data taken with a special set-up explained in the following section. The same data set is also

tested for periodicity by an independent temporal analysis [11].

The Crab Optical Pulsar

Before analyzing the gamma-ray data for periodicity, we took special runs using only the central pixel of one telescope to detect the optical pulsed signal from the Crab pulsar. This detection of the periodic optical signal confirms that our online time stamping and our offline data analysis are capable of detecting the 33 ms pulsed emission and that we can reconstruct the double-peaked phase structure of the Crab pulsar. For the special optical runs, we ran the system at the single photoelectron trigger level, triggering the system at 20 kHz and recording only the time-stamps and number of pulses collected between each trigger from the central pixel and a pixel at the outer edge of the camera. Figure 2 shows the phase plot of the signal obtained by combining the data from 3 runs taken on 2 different nights, for a total of 30 minutes. It clearly shows the main and inter pulses of the optical pulsed emission.

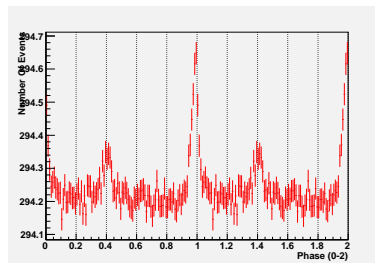


Figure 2: The phase histogram of the optical signal detected by VERITAS.

The Pulsed Emission Upper Limit

Since the pulsed emission is expected only at the lowest energies to which VERITAS is sensitive, the *Size-cut* used in the standard VERITAS analysis (Table 1) removes all relevant events. Thus, to search for the pulsed emission, all data which pass the standard quality cuts with the exception of the *Size-cut* are used. Since the angular resolution is degraded at low energy, the standard θ^2 -cut was

also relaxed to $\theta^2 < 0.04$ to enhance the acceptance of low-energy events. The binning of events by phase acts as a separation of signal and background, and no further gamma/hadron separation cuts are applied. These loose cuts increased the overall number of candidate gamma-ray events by a factor of 27.

In Figure 3 the phase histogram of the signal from the source region and the estimated background is shown for the 2-telescope data (left panels) and 3-telescope data (right panels) with the loose cuts explained in this section (upper panels) and with the standard cuts (lower panels). The significance of the pulsed excess is calculated by assuming the pulse shape as seen in the EGRET energy range, with a defined pulsed emission region between phases $[-0.06-0.04]$ and $[0.32-0.43]$ for the main pulse and inter-pulse regions respectively. The remaining phase regions are used to estimate the background for the pulsed emission. No evidence for pulsed emission is seen. An upper limit for the pulsed emission is calculated using the method of Helene [8], assuming Gaussian statistics. The upper limit in terms of the percentage of the observed DC emission is then derived separately for the 3-telescope and 2-telescope data. We will present the upper limits we have obtained at the conference.

Conclusion

Steady emission from the Crab Nebula is detected at very high significance by VERITAS. The steady signal from the Crab was used to perform various performance checks on the system for different configurations. A preliminary differential spectrum of the Crab was measured and the result is currently being compared by two independent analyses. Pulsed emission from the Crab Pulsar is also searched for with the same data set, using looser cuts. Upper limits in terms of the percentage of the DC flux were determined and will be presented at the conference.

Acknowledgments

This research is supported by grants from the U.S. Department of Energy, the U.S. National Science Foundation, the Smithsonian Institution, by

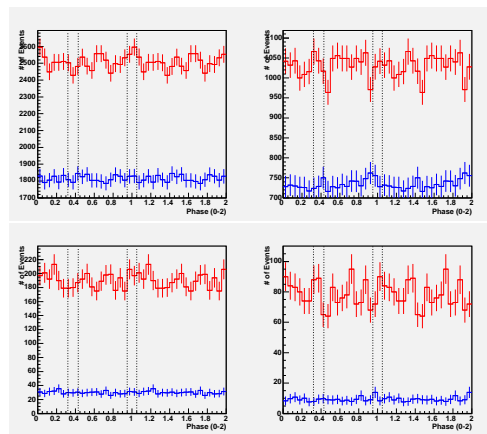


Figure 3: The phase histogram of the gamma-ray signal from the source region (red) superimposed on the estimated background from the background regions (blue) for 2-telescope (left panels) and 3-telescope (right panels) data with the loose cuts described in the text (upper panels) and with the standard cuts (lower panels).

NSERC in Canada, by PPARC in the UK and by Science Foundation Ireland.

References

- [1] A. Aharonian et al. *ApJ*, 614:897, 2004.
- [2] A. Aharonian et al. *AA*, 457:899, 2006.
- [3] P. Cogan. In *these proceedings*, 2007.
- [4] M. Daniel. In *these proceedings*, 2007.
- [5] J. K. Daugherty and A. K. Harding. *ApJ*, 458:278, 1996.
- [6] O. C. de Jager and A.K. Harding. *ApJ*, 396:161, 1992.
- [7] P. Fortin. Private communication.
- [8] O. Helene. *NIM*, 212:319, 1983.
- [9] A. M. Hillas et al. *ApJ*, 503:744, 1998.
- [10] K. Hirotani. *ApJ*, 549:495, 2001.
- [11] J. Kildea. Private communication.
- [12] A. G. Lyne, Jordan C. A., and M.E. Roberts. <http://www.jb.man.ac.uk/pulsar/crab.html>.
- [13] G. Maier. In *these proceedings*, 2007.
- [14] P. L. Nolan. *ApJ*, 409:697, 1993.
- [15] R. M. Wagner. In *The Proc. of 26th ICRC*, 2005.
- [16] T. Weekes et al. *ApJ*, 342:379, 1989.